

Impact of Solar Farm Location on Power Losses and Voltage Fluctuations in Distribution Networks Using PSCAD

Kareem Elhammamy and Hassan Nouri

School of Engineering, University of the West of England, Frenchay Campus, Bristol, United Kingdom

Kareemwalidonsy@gmail.com, hnouri2024@outlook.com

doi: 10.21608/jeatsa.2025.427796

Received 30-8-2024

Revised 14-10-2024

Accepted: 1-11-2024

Published: Jan-2025

Copyright © 2021 by author(s) and
Journal Of Engineering Advances And Technologies
Sustainable Applications
This work is licensed under the Creative
Commons Attribution International
License (CC BY 4.0).

<http://creativecommons.org/licenses/by/4.0/>



Print ISSN: 3062-5629

Online ISSN: 3062-5637

Abstract - This paper reports on the impact of PV farm location in Low-Voltage Distribution Networks (LVDNs) in terms of power loss and voltage profile.

Simulation results from a five node or bus radial network within the Power Systems Computer Aided Design (PSCAD) software, successfully demonstrate the effect of the solar farm interface at different network buses on the degree of power loss and voltage variation under three load power sizes, namely 5%, 50% and 100% of the rated power. The results also suggest that the generators' phase angle, point of coupling location, inverters and associated converters switching algorithms have great influence on the aforementioned issues. Furthermore, the injected power by the PV farm at the load side will decrease the power demand from the substation. This in turn leads to the loss reduction and voltage profile improvement within the network. However, if the PV farm power generation is more than the load demand, some power may flow towards the substation. Consequently, a voltage rise can be expected along the distribution network. The rise of the voltage limits the amount of penetration level that can be installed in the distribution networks.

Keywords – PV Farms, Distribution Networks, Power Quality

INTRODUCTION

Fossil fuel resources, due to their harmful emissions, pollution and high losses in low voltage lines, are putting great pressure on the power industry [1-2]. Although solar PVs generate clean power, their integration faces problems as their output power depends on strength of the sun irradiance [3]. Also, the excessive penetration of PV generation units will have negative impact on LVDNs behaviour [2]. Distribution networks may be considered as bidirectional systems due to the reversing power flow from the excessive connection of PVs [4] which will lead to an overvoltage challenge that occurs at the point of common coupling (PCC) [5]. Furthermore, solar irradiance may cause overloading on the components of distribution networks [6]. This may lead to an imbalanced condition between the generation and demand units [7]. All these will have an impact on the overall network performance, such as stability and efficiency [8], power quality [9], frequency oscillation [3] and subsequently the system inertia [10].

Recently Mahmud et al [11] and Samadi et al [12] have reported that small or medium-sized PV generation has the benefits of cleanliness and high efficiency.

In general, the grid-integration of large-scale PV farms has altered the operating characteristics of the traditional distribution network. For example, from unidirectional power flow to bidirectional power flow, from power sources only at the generation or substation side to power sources at both the generation and the load sides [13]. It has been reported [14]– [17] that as the location of PV farms has an impact on the network power losses and voltage fluctuations of the distribution network, obtaining the optimum location of the PV farms interface to the grid still requires further attention.

The aim of this study is to initially investigate the impact of PV farm location in a five-bus Low-Voltage Distribution Network (LVDNs) using Power Systems Computer Aided Design (PSCAD) software in terms of characteristics of the power flow, voltage profile and power loss under various test scenarios. Then to further strengthen the findings reported earlier.

CIRCUIT TOPOLOGY AND MEASUREMENT

Figure 1 shows a typical radial distribution network. Here the location of a PV farm can be varied by placing its equivalent generator at various buses. The active and reactive power, voltage fluctuation and its phase shift can be measured at each bus. The drop in the voltage and the power loss can be obtained by comparing the measured parameter with its corresponding neighbouring bus parameter.

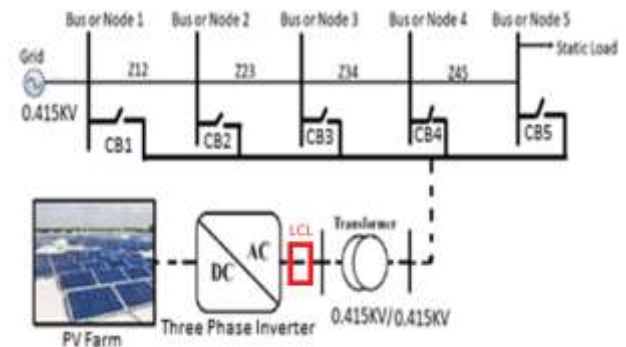


Figure 6 represents single line diagram of a typical five bus or node distribution network

I. POWER FLOW BETWEEN PV FARM AND GRID

The PV farm power is transferred to the grid through a three-phase inverter that provides active power to the load and at the same time delivers reactive power to the grid for the provision of grid voltage support.

Fig. 2 shows an equivalent impedance circuit that exists between the PV farm inverter and the grid. The active power and reactive power injected to the grid are expressed as:

$$P = \frac{1}{Z} [(V_1 V_2 \cos \phi - V_1^2) \cos \theta + V_1 V_2 \sin \phi \sin \theta] \quad (1)$$

$$Q = \frac{1}{Z} [(V_1 V_2 \cos \phi - V_1^2) \sin \theta - V_1 V_2 \sin \phi \cos \theta] \quad (2)$$

where V_1 is the voltage of the distribution grid, V_2 is the voltage of the Voltage Source Inverter (VSI), and ϕ is the phase angle between V_1 and V_2 .

If the line impedance is considered more inductive ($X \gg R$), then R is neglected and the above equations are expressed as:

$$P = \frac{V_1 V_2}{X} \sin \phi \quad (3)$$

$$Q = \frac{V_1 V_2 \cos \phi - V_1^2}{v} \quad (4)$$

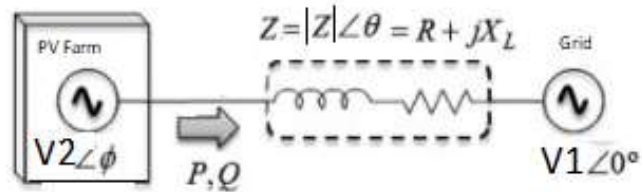


Figure 2 Power flow between the grid (V_1) and PV generator (V_2)

II. PSCAD CIRCUIT CONSTRUCTION

For steady state and transient state analysis, a simplified model of a radial distribution system with PV farm integration constructed in PSCAD is shown in Fig. 3.

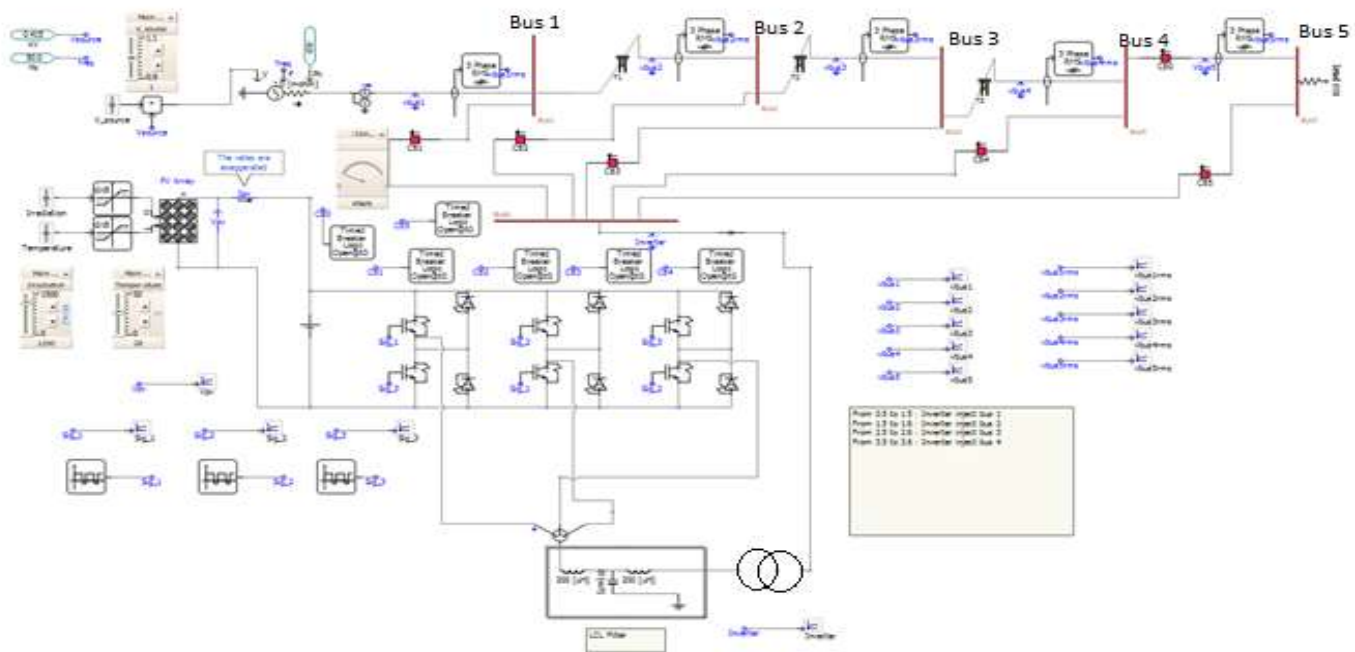


Figure 3 Simple model of radial distribution system with PV farm integration

The 415 volts generator with a resistance of $1 \text{ m } \Omega$ is a star connected three phase model. The 10 MW (rated load power) delta connected resistive load receives power from the generator via three series connected transmission line each with a length of 71 meters. Each three-phase line is divided into two sections to facilitate the fault analysis studies at various points along the lines. The PV farm, which is composed of solar panels, a three-phase inverter

and a LCL filter, is connected to each bus via a three-phase, one to one ($N_p = N_s$) transformer. The connection of the PV farm to each bus, forms a scenario. At each scenario, the angle of the grid's generator is changed to observe the characteristics of power flow (P and Q known as active and reactive power respectively), the voltage magnitude in

switches with 3 generated controlled switching signals with phase shift of 0° , 120° and 240° respectively. The LCL filter consists of 2 inductors of 200 μH each and a capacitor of 80 mF. For the purposes of PV farm output interface with the grid, the phase difference between the inverter and the main generator is kept at zero, as shown in Fig. 4.

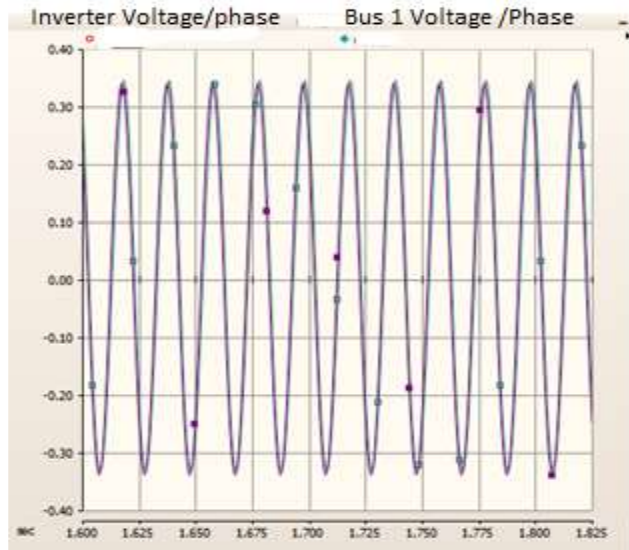


Figure 4 Three phase inverter phase test with generator

For connection of the PV farm to each bus to form scenarios, five circuit breakers are employed to operate in sequence (see Fig. 3). The first circuit breaker “CB1” injects PV farm output power into bus 1 from 0.5 to 0.6s, CB2 injects PV farm output power into bus 2 from 1.5 to 1.6s and then CB3 injects PV farm output power into bus 3 from 2.5 to 2.6s, CB4 injects PV farm output power into bus 4 from 3.5 to 3.6s and finally CB5 injects PV farm output power into bus 5 from 4.5 to 4.6s. To validate the PSCAD simulation results for the resistive loads ($\cos \phi = 1$) the following equations are used:

$$P = \sqrt{3} \times VL \times I \times \cos \phi \quad (5)$$

$$P = I^2 \times R \quad (I = I_{Line} = I_{Phase}) \quad (6)$$

$$R = \frac{V(\text{phase})}{I} \quad (7)$$

The three different, three-phase resistive load sizes are 10 MW (100% rated power), 5 MW (50% rated power) and 500 KW (5% rated power) which draw three different currents that affects the power loss, the bus voltage and the angle magnitude within the grid.

I. RESULTS AND DISCUSSION

The reference voltage at each bus and the reference power loss between the two successive buses are measured when no PV farm is connected to the grid. Further measurement is performed at various points within the network of Fig. 1 or Fig. 3 following the test procedures mentioned earlier for the formation of various scenarios. As an example, figure 5 shows the per unit value of the bus 3 voltage under different scenarios.

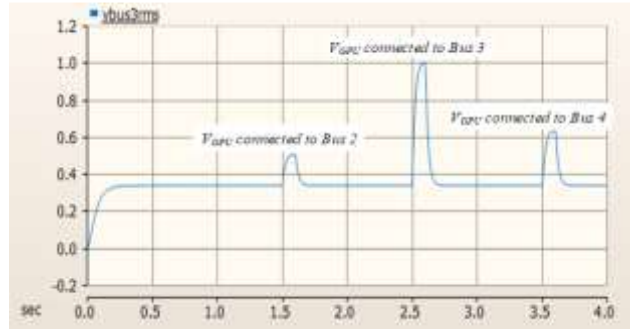


Figure 5 shows the per unit voltage of Bus 3 (V3) when the output of the PV Inverter (V_{GPV}) is connected to various buses

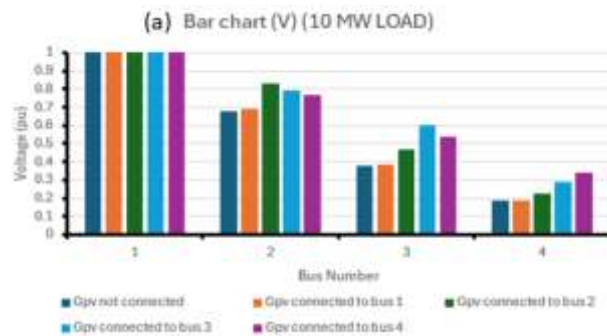
Table 1 shows the per unit voltage of various Buses when the output of the PV Inverter (V_{GPV}) is connected to various buses under a 50% load condition.

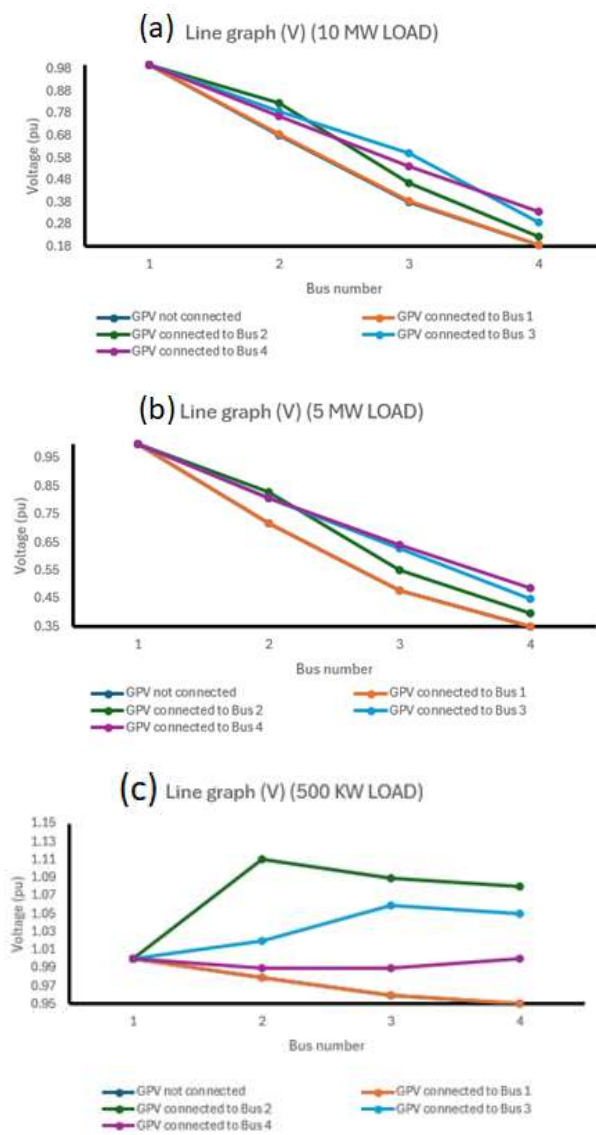
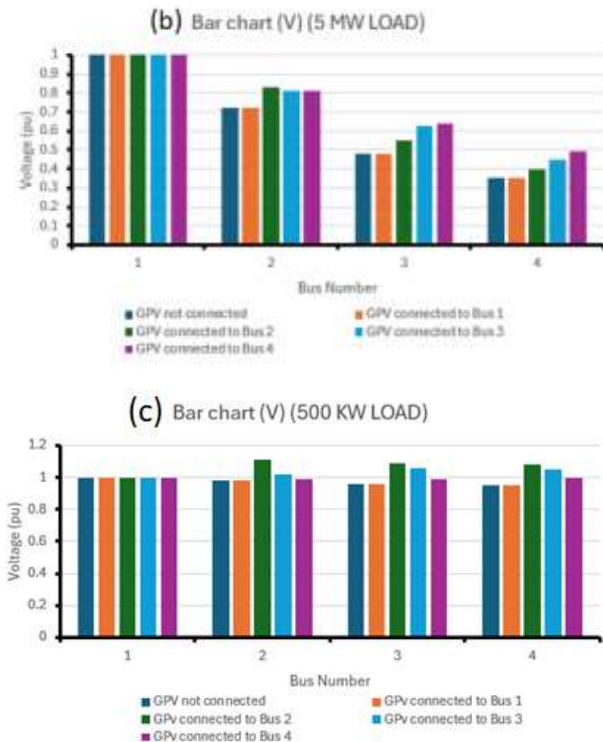
Table 1 the sequence effect of PV output (V_{GPV}) interface to various buses under a 50% load condition

Time	V_{GPV} connection	v1	v2	v3	v4
0.3 s	No bus	1 (PU)	0.67 (pu)	0.33 (pu)	0.003 (pu)
0.5-0.6 s	to bus 1	1	0.67	0.33	0.003
1.5-1.6 s	to bus 2	1	1	0.5	0.0045
2.5-2.6 s	to bus 3	1	1	1	0.009
3.5-3.6 s	to bus 4	1	0.81	0.63	0.442

Furthermore, the results shown in table 1 are represented by bar charts and line graphs for ease of analysis and discussion.

Figures 6 shows the bar chart per unit of the bus voltages for the scenarios discussed in table 1 for three different resistive load sizes, namely: (a) 10 MW (100% rated power), (b) 5 MW (50% rated power) and (c) 500 KW (5% rated power).





Figures 6 Bar chart per unit representation of the bus voltages for the scenarios discussed in table 1 for three different resistive load sizes namely: (a) 10 MW (100%), (b) 5 MW (50%) and (c) 500 KW (5%).

The corresponding lined graphs representation of bar charts are shown in Fig. 7.

Figures 7 Line graphs per unit representation of the bus voltages for the scenarios discussed in table 1 for three different resistive load sizes namely: (a) 10 MW (100%), (b) 5 MW (50%) and (c) 500 KW (5%).

Tentative analysis of the presented results reveals that in the absence of PV farm interface with the grid, a significant loss appears across the grid. This is especially pronounced at the load side where the load bus voltage is close to zero. However, less loss is observed when the PV farm is connected to Bus 3 or Bus 4. However, this difference is significant at 500 KW (5%) resistive load.

Figure 8 and figure 9 depict the Bar chart and the line graphs KW representation of the power loss respectively for the scenarios discussed in table 1 under three different resistive load sizes, namely: (a) 10 MW (100%), (b) 5 MW (50%) and (c) 500 KW (5%).

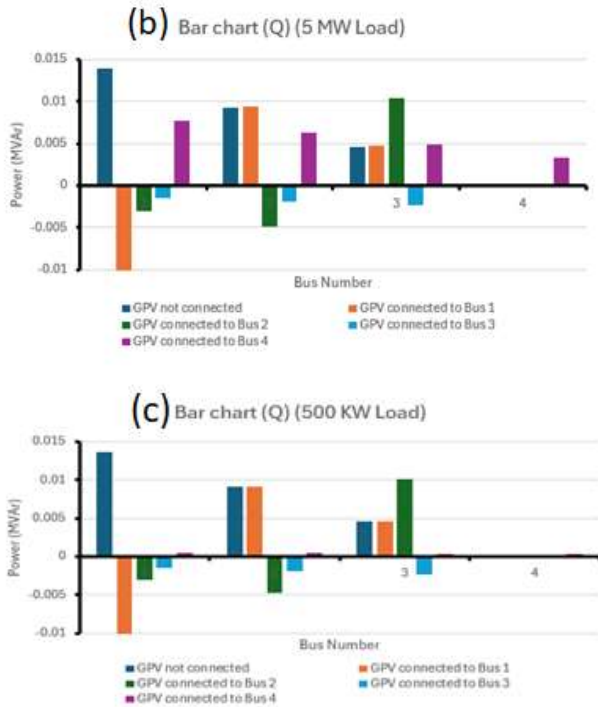


Figure 10 shows the bar charts in MVA representation of the reactive power loss for the scenarios discussed in table 1 under three different resistive load sizes namely: (a) 10 MW (100%), (b) 5 MW (50%) and (c) 500 KW (5%).

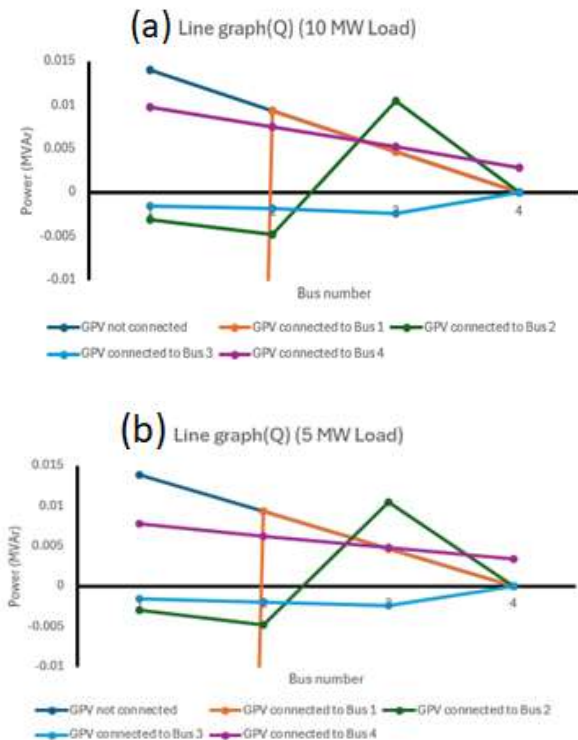


Figure 11 shows the line graph in MVA representation of the reactive power loss for the scenarios discussed in table 1 under three different resistive load sizes namely: (a) 10 MW (100%), (b) 5 MW (50%) and (c) 500 KW (5%).

I. CONCLUSIONS

This study highlights the crucial significance of photovoltaic (PV) farm location within low-voltage distribution networks (LVDNs) in optimizing network efficiency and power quality. Through meticulous simulations conducted using PSCAD software, it is evident that the placement of PV farms has a substantial impact on various parameters including power loss, voltage magnitude, and voltage angle, particularly under various load sizes. The analysis identified Bus 4 as the optimal location for PV farm connection, representing the right side of the network closest to the load. However, recognizing the practical constraints associated with this proximity to populated areas, Bus 3 emerges as the more feasible choice. This location strikes a balance between technical optimization and real-world considerations, ensuring efficient power distribution while addressing practical concerns. In the next stage of the work, combined meshed and radial networks with more PV farms penetration to the grid will be studied in conjunction with available optimisation techniques and AI.

REFERENCES

- [1] Fasihi M, Weiss R, Savolainen J, Breyer C. Global potential of Green ammonia based on hybrid PV-wind power plants. *Appl Energy*. 2021; 294:116170.
- [2] Hashemi M, Østergaard J. Methods and strategies for overvoltage prevention in low voltage distribution systems with PV. *IET Renewable Power Gener*. 2017; 11:205-214.
- [3] Behura A, Kumar A, Rajak D, Pruncu C, Lambert L. Towards better performances for a novel rooftop solar PV system. *Sol Energy*. 2021; 216:518-529.
- [4] Holguin J, Celeita D, Ramos G. Reverse power flow (RPF) detection and impact on protection coordination of distribution systems. *IEEE Trans Ind Appl*. 2019; 56(4):2393-2401.
- [5] Zeraati M, Golshan M, Guerrero J. Voltage quality improvement in low voltage distribution networks using reactive power capability of single-phase PV inverters. *IEEE Trans Smart Grid*. 2018; 10(5):5057-5065.
- [6] Luo C, Wu H, Zhou Y, Qiao Y, Cai M. Network partition-based hierarchical decentralized voltage control for distribution networks with distributed PV systems. *Int J Electr Power Energy Syst*. 2021; 130:106929.

-] Vergara P, Salazar M, Mai T, Nguyen P, Slootweg H. A comprehensive assessment of PV inverters operating with droop control for overvoltage mitigation in LV distribution networks. *Renew Energy*. 2020; 159:172 -183.
- [8] Islam M, Mithulananthan N, Hossain J, Shah R. Dynamic voltage stability of unbalanced distribution system with high penetration of single-phase PV units. *J Eng*. 2019;2019 (17):4074 -4080.
- [9] De Silva H, Jayamaha D, Lidula N. Power Quality Issues Due to High Penetration of Rooftop Solar PV in Low Voltage Distribution Networks: A Case Study. Paper presented at: 14th Conference on Industrial and Information Systems (ICIIS). 20 19; Kandy, Sri Lanka, Sri Lanka, 18 - 20.
- [10] Adrees A, Milanovi_c J, Mancarella P. Effect of inertia heterogeneity on frequency dynamics of low -inertia power systems. *IET Gener Transm Distrib*. 2019;13(14):2951 - 2958.
- [11] N. Mahmud and A. Zahedi, "Review of control strategies for voltage regulation of the smart distribution network with high penetration of renewable distributed generation," *Renewable and Sustainable Energy Reviews* , vol. 64, pp. 582 -595, Oct. 2016.
- [12] A. Samadi, R. Eriksson, L. Söder, B. G. Rawn, and J. C. Boemer, "Coordinated active power -dependent voltage regulation in distribution grids with PV systems," *IEEE Transactions on Power Delivery* , vol. 29, no. 3, pp. 1454 - 1464, Jun. 2014.
- [13] M. Y. Shih, A. Conde, Z. Leonowicz, and L. Martirano, "An adaptive overcurrent coordination scheme to improve relay sensitivity and overcome drawbacks due to distributed generation in smart grids," *IEEE Transactions on Industry Applications* , vol. 53, no. 6, pp. 5217 -5228, Nov. /Dec. 2017.
- [14] F. Olivier, P. Aristidou, D. Ernst, and T. Van Cutsem, "Active management of low -voltage networks for mitigating overvoltages due to photovoltaic units," *IEEE Transactions on Smart Grid* , vol. 7, no. 2, pp. 926 -936, Mar. 2016.
- [15] Y. V. P. Kumar and R. Bhimasingu, "Renewable energy based microgrid system sizing and energy management for green buildings," *Journal of Modern Power Systems and Clean Energy* , vol 3, no. 1, pp. 1 -13, Mar. 2015.
- [16] J. Liu, Y. Miura, and T. Ise, "Comparison of dynamic characteristics between virtual synchronous generator and droop control in inverter based distributed generators," *IEEE Transactions on Power Electronics* , vol. 31, no. 5, pp. 3600 -3611, May. 2016.
- [17] H. X. Zhan, C. S Wang, Y. Wang, X. H. Yang, X. Zhang, C. J. Wu, and Y. H. Chen, "Relay protection coordination integrated optimal placement and sizing of distributed generation sources in distribution networks," *IEEE Transactions on Smart Grid* , vol. 7, no. 1, pp. 55-65, Jan. 2016.